

# Supplementary material of “R2-based Hypervolume Contribution Approximation”

Ke Shang, Hisao Ishibuchi, *Fellow, IEEE*, and Xizi Ni

## APPENDIX A

### EXPLANATIONS ON THE MONTE CARLO METHOD

Here we give some detailed examples to clearly explain why the Monte Carlo method is able to achieve a good performance on the triangular PF solution sets when  $r = 0.0$  while its performance deteriorates dramatically when  $r = -0.1, \dots, -0.4$ .

We pick three solution sets (say, solution sets 1, 2, 3) from the linear triangular PF solution sets for illustration. Fig. 1-3 show the informations of the solution sets 1-3 respectively. In each figure, the above two subfigures show the information of the solution set when  $r = 0.0$ , while the below two subfigures show the information of the solution set when  $r = -0.1$ . The subfigures on the left are the parallel coordinate plots of the solutions in the solution set, and the subfigures on the right show the relations between the hypervolume contribution and the sampling space size of the solutions in the solution set. The solution with the smallest hypervolume contribution is highlighted through the red line on the left and red circle on the right.

From the figures we can see that when  $r = 0.0$ , the solution with the smallest hypervolume contribution is close to or lie on the boundaries of the PF (i.e., at least one objective value is close to or equal to 0), and this solution also tends to have the smallest sampling space size among all the solutions. However, when  $r = -0.1$ , the solution with the smallest hypervolume contribution lies inside of the PF (i.e., all objective values are not close to or equal to 0), and this solution does not have the smallest sampling space size among all the solutions.

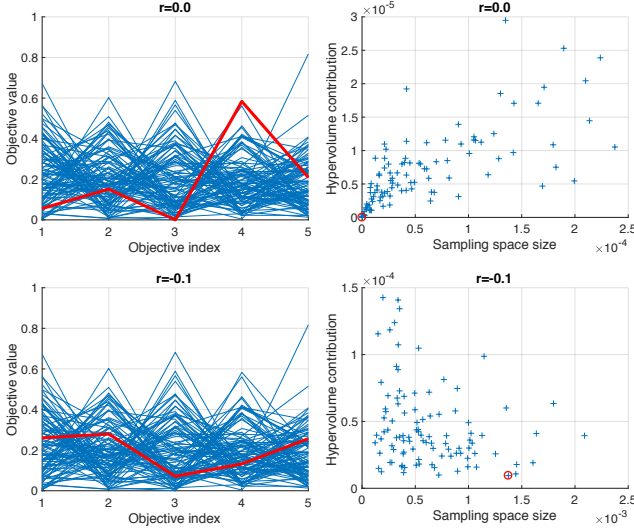


Fig. 1. Solution set 1 of the linear triangular PF solution sets

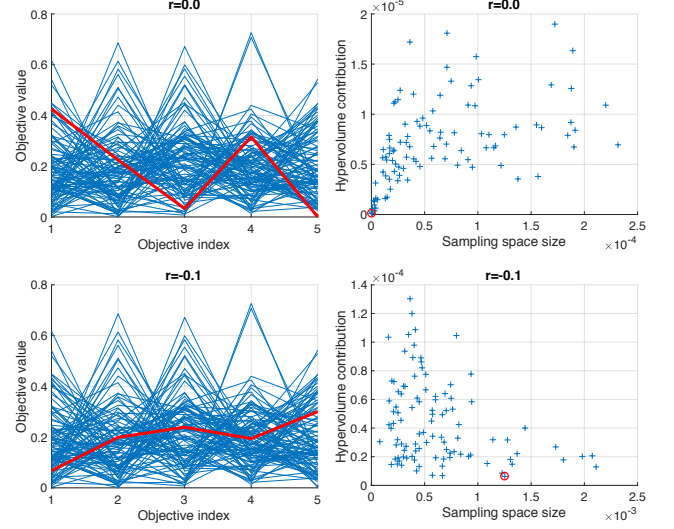


Fig. 2. Solution set 2 of the linear triangular PF solution sets

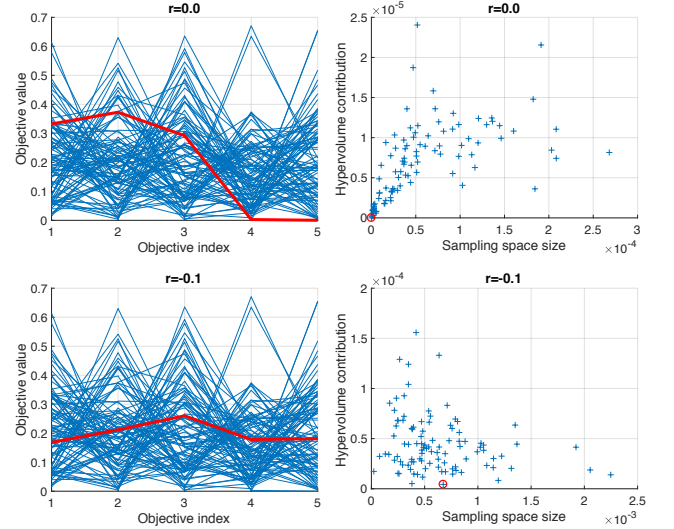


Fig. 3. Solution set 3 of the linear triangular PF solution sets

The Monte Carlo method first determines the tightest sampling space, then approximates the hypervolume contribution based on this sampling space. Therefore, the performance of the Monte Carlo method strongly depends on the sampling space. When  $r = 0.0$ , the solution with the smallest hypervolume contribution tends to have the smallest sampling space size, which makes the Monte Carlo method easy to identify it. When  $r = -0.1$ , the solution with the smallest hypervolume contribution does not have the smallest sampling

space size, and there exist many other solutions with much smaller sampling space size, which makes the Monte Carlo method difficult to identify it. We can get similar observations for  $r = -0.2, -0.3, -0.4$  to the case of  $r = -0.1$ .

From the above analysis we can see that the performance of the Monte Carlo method is sensitive to the specification of the reference point, which is the main drawback of the Monte Carlo method compared with the proposed method in this paper. As suggested in [1], appropriate reference point specification is essential in the hypervolume-based EMOAs for fair performance comparison. The Monte Carlo method is not practical because it only performs well on the triangular PF solution sets with  $r = 0.0$ , and generally this is not a good choice for the reference point specification.

## APPENDIX B

### RESULTS ON 10-DIMENSION SOLUTION SETS

The results of the two performance metrics on 10-dimension solution sets are shown in Fig. 4-9. All the results in the figures are the average of 30 independent runs with different seeds in the generation of the direction vectors and the sampling points.

For the triangular PF solution sets (see Fig. 4-6), we can observe that the new method always outperforms the traditional method in terms of both performance metrics. When the reference point  $r = 0.0$ , the Monte Carlo method shows the best performance, while its performance deteriorates dramatically as the reference point changes from 0.0 to -0.4. The new method shows a robust performance with respect to the specification of the reference point. In most cases (except for the case of concave triangular PF solution sets), its performance is worse than the Monte Carlo method only when  $r = 0.0$ , while it outperforms the Monte Carlo method when  $r = -0.1, \dots, -0.4$ . For the concave triangular PF solution sets (see Fig. 6), the Monte Carlo method shows a better performance when  $r = 0.0, -0.1, -0.2$ , while its performance is worse than the new method when  $r = -0.4$ . We can expect that the performance of the Monte Carlo method will continue to decrease as the reference point moves further.

For the Inverted Triangular PF solution sets (see Fig. 7-9), we can observe that the new method always outperforms the traditional method and the Monte Carlo method in terms of both performance metrics. We can also see that the new method achieves a robust performance with respect to the specification of the reference point.

From the experimental results we can see that the new method is able to achieve a good and robust performance even when the number of the direction vectors is small (e.g., 100). The performance of the Monte Carlo method strongly depends on the shape of the PF and the specification of the reference point. Its performance deteriorates dramatically as the reference point moves further. For this reason, the new method is more practical and reliable in the hypervolume-based EMOAs.

## REFERENCES

- [1] H. Ishibuchi, R. Imada, Y. Setoguchi, and Y. Nojima, "How to specify a reference point in hypervolume calculation for fair performance comparison." *Evolutionary Computation*, vol. 26, no. 3, pp. 411–440, 2018.

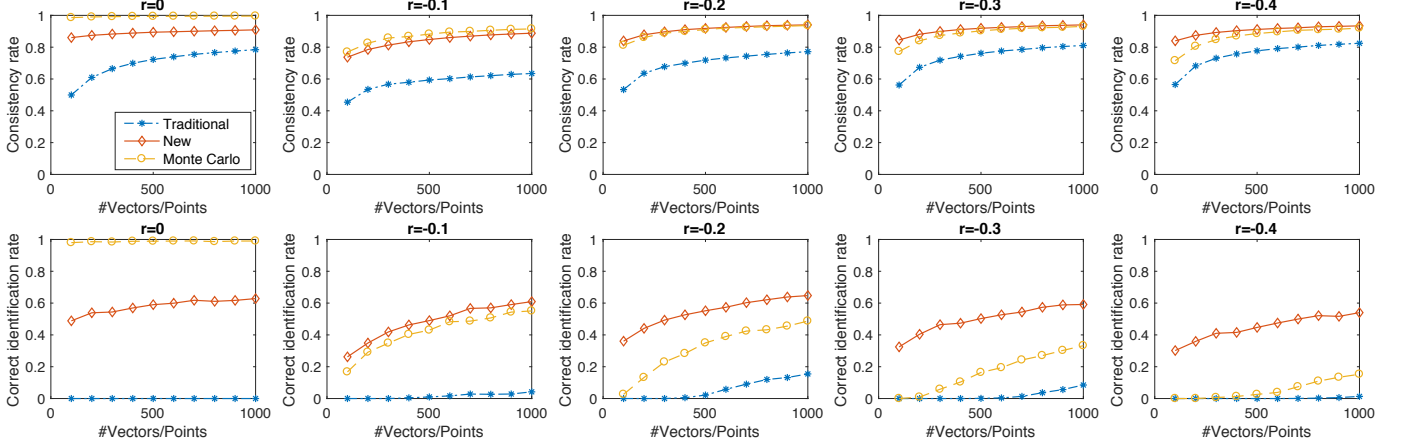


Fig. 4. Results on the 10-dimension linear triangular PF solution sets.

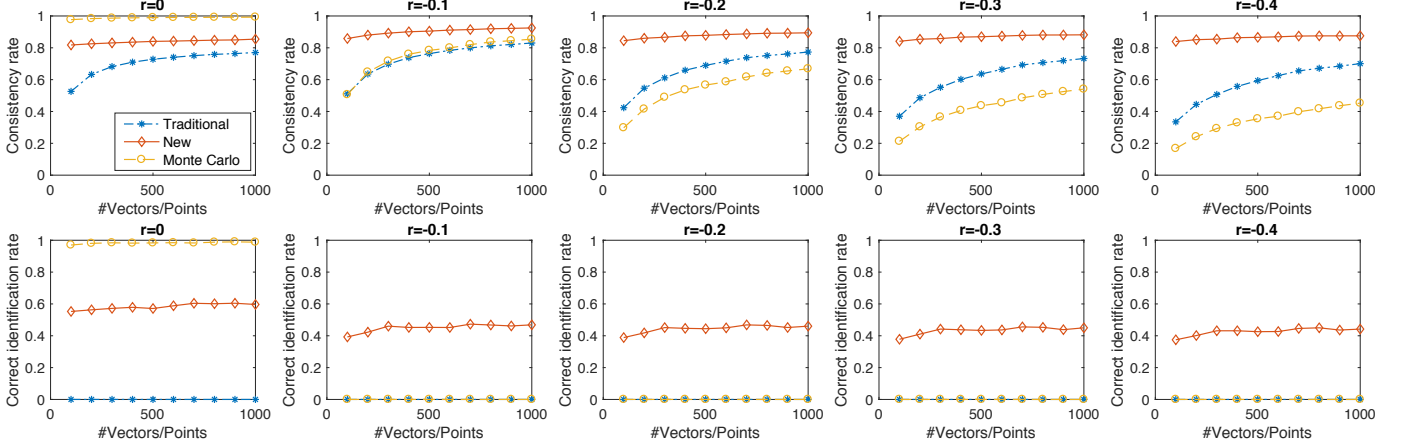


Fig. 5. Results on the 10-dimension convex triangular PF solution sets.

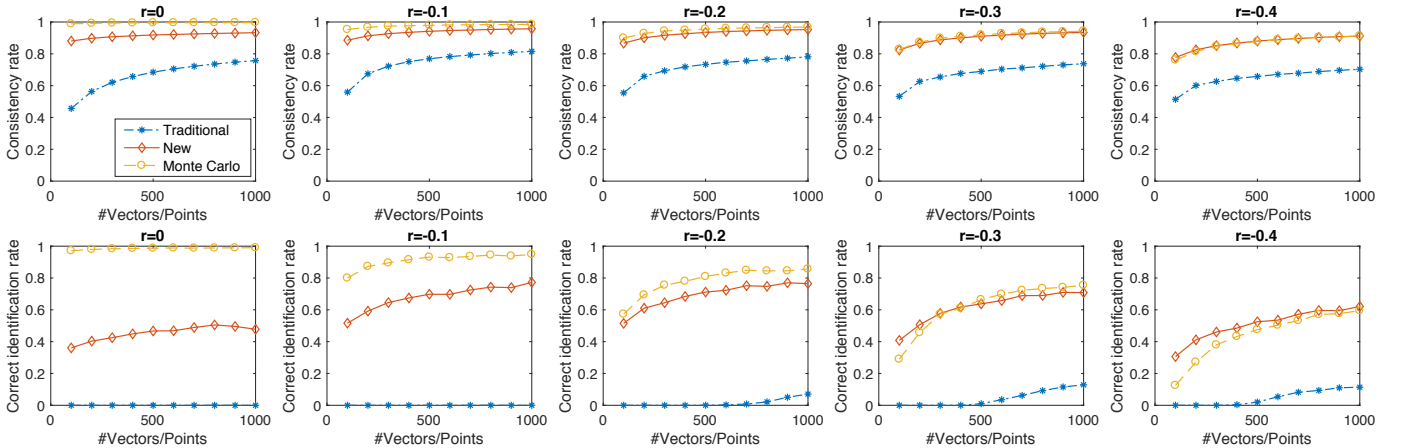


Fig. 6. Results on the 10-dimension concave triangular PF solution sets.

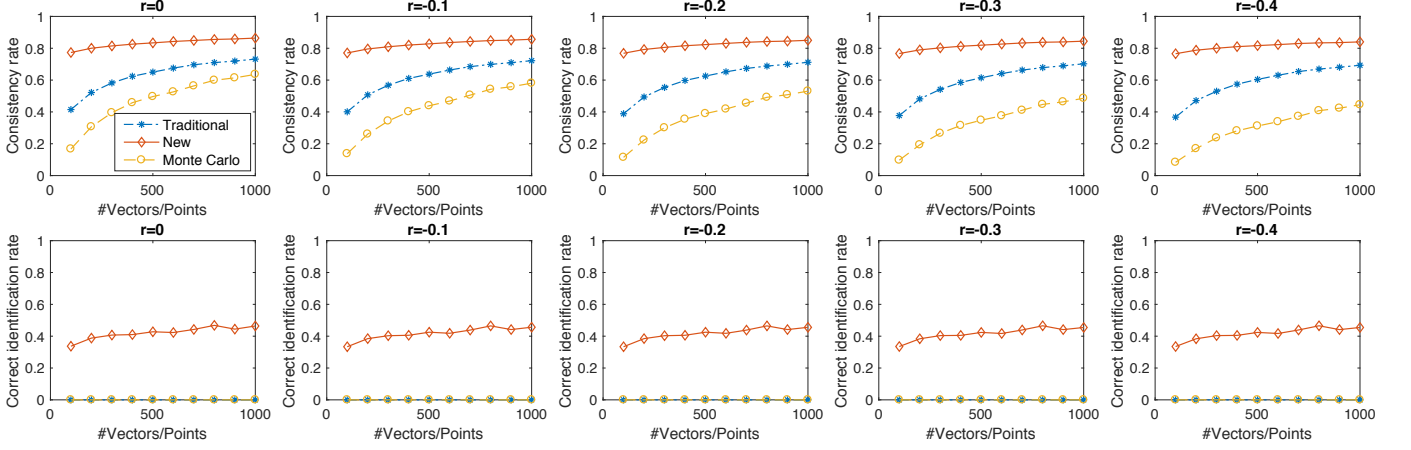


Fig. 7. Results on the 10-dimension linear inverted triangular PF solution sets.

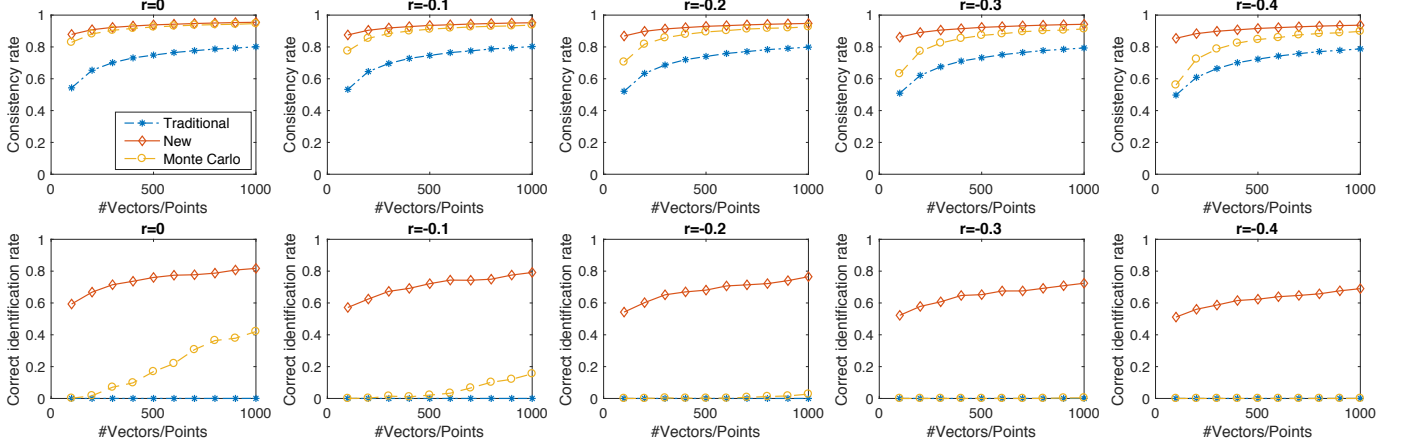


Fig. 8. Results on the 10-dimension convex inverted triangular PF solution sets.

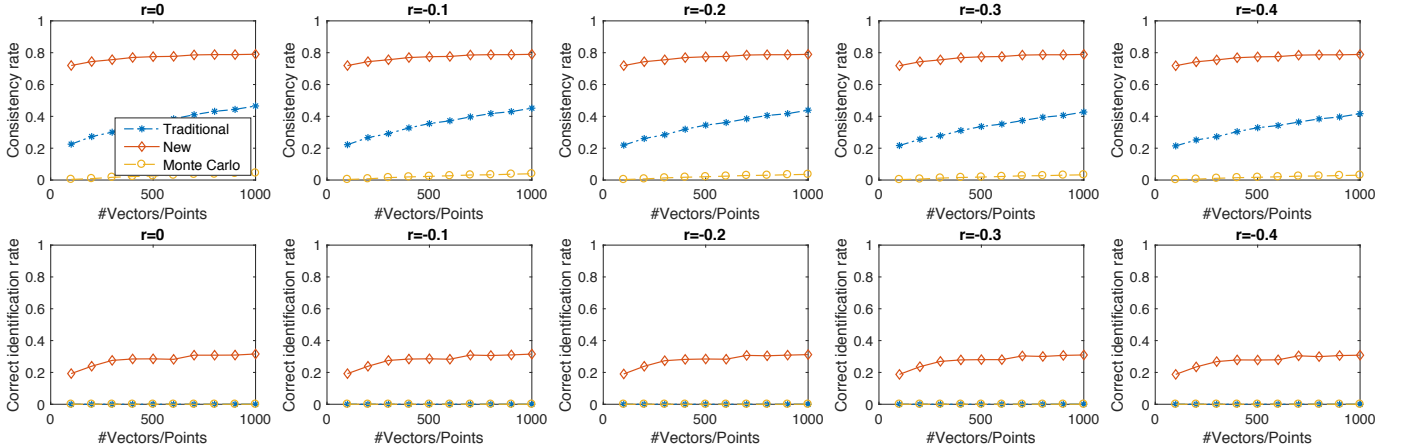


Fig. 9. Results on the 10-dimension concave inverted triangular PF solution sets.